



A *Ralstonia solanacearum* type III effector directs the production of the plant signal metabolite trehalose-6-phosphate

Marie Poueymiro, Anne-Claire Cazalé, Jean-Marie François, Jean-Luc Parrou, Nemo Peeters, Stéphane Genin

► To cite this version:

Marie Poueymiro, Anne-Claire Cazalé, Jean-Marie François, Jean-Luc Parrou, Nemo Peeters, et al.. A *Ralstonia solanacearum* type III effector directs the production of the plant signal metabolite trehalose-6-phosphate. *mBio*, American Society for Microbiology, 2014, 5 (6), pp.1-9. <10.1128/mBio.02065-14>. <hal-01133638>

HAL Id: hal-01133638


<https://hal.archives-ouvertes.fr/hal-01133638>

Submitted on 19 Nov 2015

HAL is a multi-disciplinary open access archive for the deposit and dissemination of scientific research documents, whether they are published or not. The documents may come from teaching and research institutions in France or abroad, or from public or private research centers.

L'archive ouverte pluridisciplinaire **HAL**, est destinée au dépôt et à la diffusion de documents scientifiques de niveau recherche, publiés ou non, émanant des établissements d'enseignement et de recherche français ou étrangers, des laboratoires publics ou privés.

A *Ralstonia solanacearum* Type III Effector Directs the Production of the Plant Signal Metabolite Trehalose-6-Phosphate

M. Poueymiro,^{a,b,*} A. C. Cazalé,^{a,b} J. M. François,^{c,d,e} J. L. Parrou,^{c,d,e}  N. Peeters,^{a,b} S. Genin^{a,b}

INRA, Laboratoire des Interactions Plantes-Microorganismes (LIPM), UMR441, Castanet-Tolosan, France^a; CNRS, Laboratoire des Interactions Plantes-Microorganismes (LIPM), UMR2594, Castanet-Tolosan, France^b; Université de Toulouse, INSA, UPS, INP, LISBP, Toulouse, France^c; INRA, UMR792, Ingénierie des Systèmes Biologiques et des Procédés, Toulouse, France^d; CNRS, UMR5504, Toulouse, France^e

* Present address: The Lycée Raoul Dautry, Limoges, France.

M.P. and A.C.C. and N.P. and S.G. contributed equally to this article.

ABSTRACT The plant pathogen *Ralstonia solanacearum* possesses two genes encoding a trehalose-6-phosphate synthase (TPS), an enzyme of the trehalose biosynthetic pathway. One of these genes, named *ripTPS*, was found to encode a protein with an additional N-terminal domain which directs its translocation into host plant cells through the type 3 secretion system. RipTPS is a conserved effector in the *R. solanacearum* species complex, and homologues were also detected in other bacterial plant pathogens. Functional analysis of RipTPS demonstrated that this type 3 effector synthesizes trehalose-6-phosphate and identified residues essential for this enzymatic activity. Although trehalose-6-phosphate is a key signal molecule in plants that regulates sugar status and carbon assimilation, the disruption of *ripTPS* did not alter the virulence of *R. solanacearum* on plants. However, heterologous expression assays showed that this effector specifically elicits a hypersensitive-like response on tobacco that is independent of its enzymatic activity and is triggered by the C-terminal half of the protein. Recognition of this effector by the plant immune system is suggestive of a role during the infectious process.

IMPORTANCE *Ralstonia solanacearum*, the causal agent of bacterial wilt disease, infects more than two hundred plant species, including economically important crops. The type III secretion system plays a major role in the pathogenicity of this bacterium, and approximately 70 effector proteins have been shown to be translocated into host plant cells. This study provides the first description of a type III effector endowed with a trehalose-6-phosphate synthase enzymatic activity and illustrates a new mechanism by which the bacteria may manipulate the plant metabolism upon infection. In recent years, trehalose-6-phosphate has emerged as an essential signal molecule in plants, connecting plant metabolism and development. The finding that a bacterial pathogen could induce the production of trehalose-6-phosphate in plant cells further highlights the importance of this metabolite in multiple aspects of the molecular physiology of plants.

Received 1 October 2014 Accepted 20 November 2014 Published 23 December 2014

Citation Poueymiro M, Cazalé AC, François JM, Parrou JL, Peeters N, Genin S. 2014. A *Ralstonia solanacearum* type III effector directs the production of the plant signal metabolite trehalose-6-phosphate. *mBio* 5(6):e02065-14. doi:10.1128/mBio.02065-14.

Invited Editor Daniela Buettner, Martin Luther University Halle-Wittenberg **Editor** Regine Kahmann, MPI for Terrestrial Microbiology

Copyright © 2014 Schulz et al. This is an open-access article distributed under the terms of the [Creative Commons Attribution-NonCommercial-ShareAlike 3.0 Unported license](https://creativecommons.org/licenses/by-nc-sa/4.0/), which permits unrestricted noncommercial use, distribution, and reproduction in any medium, provided the original author and source are credited.

Address correspondence to N. Peeters, nemo.peeters@toulouse.inra.fr, or S. Genin, stephane.genin@toulouse.inra.fr.

Ralstonia solanacearum is a soilborne plant-pathogenic beta-proteobacterium with a wide host range and a wide geographic distribution (1). Plants from more than 50 botanical families, including major agricultural crops, are affected by this bacterial wilt disease. As a root and vascular pathogen, *R. solanacearum* is a model system to investigate the molecular mechanisms of bacterial pathogenicity (2, 3). Among the many virulence determinants that have been identified, the type III secretion system (T3SS) is essential to *R. solanacearum* pathogenesis. This T3SS machinery was shown to deliver a large set of 70 to 75 effector proteins directly into the cytoplasm of plant cells (4–7). A classification of type III effector (T3E) genes found in the *R. solanacearum* species complex using a unified nomenclature was recently proposed (4). The expression of the T3SS and T3E genes is under the transcriptional control of the *hrpB* regulatory gene (8). Excluding rare cases on specific hosts (9, 10) disruption of

single T3E genes does not significantly alter disease symptom development, and this certainly reflects the synergistic and overlapping functions of the T3Es in *R. solanacearum* pathogenicity. Cumulative disruption of T3E could indeed lead to disease symptom reduction (9, 11) or reduced multiplication *in planta* (12). Some single T3E mutant strains were also reported to have reduced levels of multiplication *in planta* compared to their multiplication in the wild type when used in competitive assays (13).

T3Es can also betray the pathogen by triggering a defense reaction from the plant immune system if the plant possesses a resistance protein able to specifically recognize one of these T3Es (14). Several of these T3Es, formerly called “avirulence” determinants, have been characterized in *R. solanacearum* (3). RipP1 (formerly known as PopP1), RipP2 (PopP2), and RipAX2 (Rip36) are avirulence determinants triggering resistance on petunia, *Arabidopsis*, and eggplant lines, respectively (15–17). On tobacco species, two

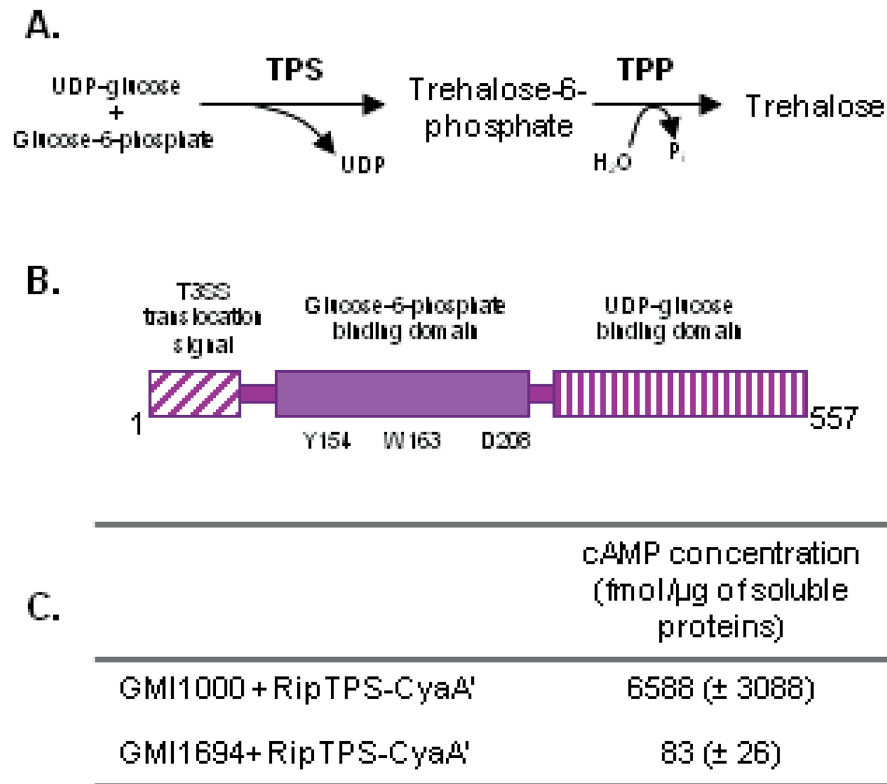


FIG 1 *ripTPS* encodes a T3E homologous to trehalose phosphate synthases. (A) Enzymatic reactions catalyzed by trehalose-6-phosphate synthase (TPS) and trehalose-6-phosphate phosphatase (TPP) in the trehalose biosynthetic pathway. (B) Schematic representation of RipTPS functional domains and some of the conserved residues predicted to be essential for activity. (C) The concentrations of cyclic AMP (cAMP) were measured in *N. tabacum* leaves after infiltration of *R. solanacearum* strains with or without a functional T3SS (GMI1000 and *hrcV*, respectively) expressing the RipTPS N-terminal domain (first 88 amino acids) fused to the calmodulin-dependent adenylate cyclase. Standard errors of the results of three independent experiments are shown in brackets.

T3Es in *R. solanacearum* strain GMI1000, RipAA (AvrA) and RipP1, elicit a hypersensitive reaction (HR), a localized and programmed cell death at the sites of infection. The double inactivation of *ripAA* and *ripP1* is sufficient to restore pathogenicity, showing that both determinants restrict the host range of *R. solanacearum* on *Nicotiana* spp. (18).

The molecular function of most *R. solanacearum* T3Es once inside plant cells remains elusive. Many T3Es do not have homology with proteins of known function, and relatively few functional studies have been conducted (10–12). There is evidence that RipP2 displays acetyltransferase activity (19), whereas the RipG (GALA) effector family was shown to interact with plant SKP1-like proteins, presumably acting as active components of the host ubiquitination machinery to subvert plant immunity (9, 20, 21). In addition, *R. solanacearum* possesses a transcription activator-like effector named RipTAL that is likely to promote disease through the transcriptional activation of host genes, as shown for *Xanthomonas* spp. (22, 23).

In this study, we identified and characterized a novel T3E from *R. solanacearum* strain GMI1000 that displays homology to trehalose-6-phosphate synthases, a class of enzymes that are ubiquitous in prokaryotes and eukaryotes. Complementation assays in yeast were used to demonstrate its biochemical activity and identify essential residues for enzymatic function. Interestingly, trehalose-6-phosphate has recently emerged as an essential signal molecule in plants, connecting plant metabolism and develop-

ment (24). Heterologous expression assays also show that this T3E is specifically inducing an HR-like response in tobacco.

RESULTS

RipTPS encodes an effector protein homologous to trehalose phosphate synthases and is translocated into plant cells by the T3SS. The RSp0731 gene product displays homology with proteins of the glycosyltransferase superfamily that possess a trehalose-6-phosphate synthase (TPS) activity. TPS catalyzes the transfer of glucose from UDP-glucose to glucose-6-phosphate, forming trehalose-6-phosphate (Tre6P) and UDP (Fig. 1). RSp0731 encodes a 557-amino acid (aa) protein that has 39 and 45% identity with OtsA from *Escherichia coli* and *R. solanacearum*, respectively. *E. coli* OtsA is a TPS enzyme for which a tridimensional structure was determined and on which residues required for its TPS activity have been identified (25, 26). All of the latter key residues required for substrate binding are conserved in RSp0731 (see Fig. S1 in the supplemental material). A striking difference between the RSp0731 protein and other bacterial TPS enzymes is that it carries a 77-aa N-terminal extension (Fig. S1) harboring the typical amino acid composition bias that characterizes effectors translocated through the T3SS (8). In order to demonstrate that this N-terminal domain directs the translocation of RSp0731 into plant cells through the T3SS, we used the adenylate cyclase (CyaA) assay already used in *R. solanacearum* (5, 6) that relies on the CyaA domain of the *Bordetella pertussis* cyclolysin

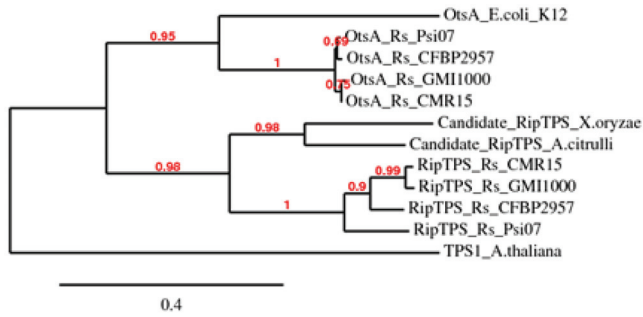


FIG 2 Bacterial TPS phylogeny. The accession numbers of the proteins aligned in this phylogeny can be found in the legend to Fig. S1 in the supplemental material. The outgroup *Arabidopsis thaliana* TPS1 (accession number NP_177979) was added in this analysis. Sequences were aligned with MUSCLE and curated with GBlocks, and the phylogeny was reconstructed with PhyML. All analysis was run using the <http://phylogeny.fr> webserver (58). Bootstrap values are indicated in red. Scale is number of substitutions per site.

(27). A chimeric protein fusion consisting of the 83 N-terminal residues from RSp0731 fused to CyaA was engineered on a plasmid vector and introduced into the wild-type strain GMI1000 and the T3SS (*hrcV*) mutant derivative GMI1694. The cyclic AMP (cAMP) concentration was monitored in tobacco plant tissue following infiltration with these strains, and the results shown in Fig. 1C indicate that this value was 73-fold higher in the wild-type strain than in the T3SS mutant. This shows that the RSp0731 N-terminal domain allows T3SS-dependent translocation into host cells; RSp0731 was therefore renamed RipTPS, in agreement with the new nomenclature (4).

***ripTPS* is a conserved effector in the *R. Solanacearum* species complex, and homologues are present in other bacterial plant pathogens.** Because the RipTPS effector is translocated into plant cells, we investigated the phylogenetic relationship of the protein with other bacterial TPS sequences. As the plant TPS is clearly an outgroup in this phylogenetic reconstruction (Fig. 2), it seems that the *R. solanacearum ripTPS* most probably originated from a duplication of a bacterial *otsA* gene. Further comparative genomic analyses show that *ripTPS* is widely conserved in strains of the *R. solanacearum* species complex. Indeed, it is present in each of the four main phylotypes, with the exception of *Ralstonia syzygii* and blood disease bacterium strains, which are undergoing a reductive genomic evolution (28) and presumably have lost the gene. All these RipTPS homologues display a high level of protein sequence identity (from 76 to 99%) among the various strains. Interestingly, in most of the strains, *ripTPS* is physically associated on the genome with another type III effector gene (*ripAV*), contrary to the other (*otsA*) TPS genes, which are physically associated with a trehalose-6-phosphate phosphatase (*otsB*)-related gene. In order to identify RipTPS effector homologues in other bacterial pathogens, we performed BLAST searches and detected proteins in *Xanthomonas oryzae* pv. *oryzae* and *Acidovorax citrulli* with a RipTPS architecture, i.e., a TPS domain and an approximately 100-aa N-terminal extension potentially involved in T3SS export (Fig. 2; also Fig. S1 in the supplemental material). This suggested that RipTPS-like effectors may be present in other vascular plant pathogens.

Functional complementation of a yeast *tps*-defective mutant by *R. solanacearum ripTPS*. In *Saccharomyces cerevisiae*, trehalose is synthesized by a TPS enzyme encoded by *tps1* and a

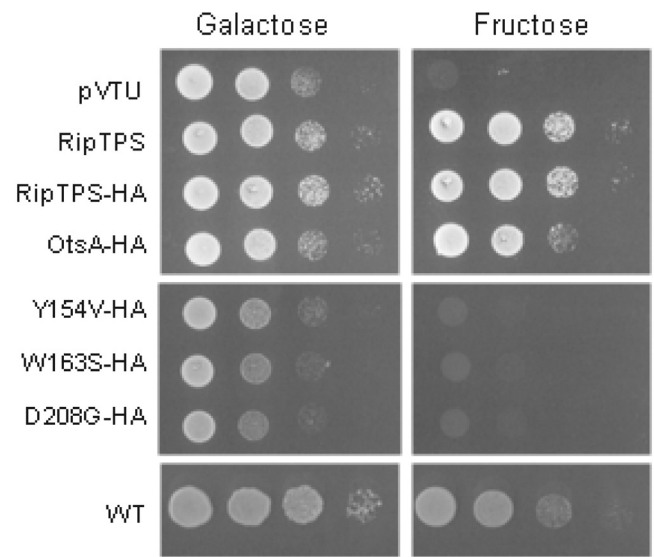


FIG 3 Complementation of the growth defect of the *S. cerevisiae tps1 tps2* strain on fructose by *R. solanacearum ripTPS*. RipTPS with or without an HA tag was expressed in the *tps1 tps2* yeast mutant, and the growth of the strain was compared to that of strains carrying an empty vector or expressing *E. coli* OtsA with an HA tag or one of the three catalytic mutants of RipTPS (Y154V, W163S, and D208G) with an HA tag. Amounts of 5 μ l of liquid cultures were spotted as a series of 10-times dilutions on 2% galactose or 2% fructose SD-LWU plates. The control yeast strain (WT) was grown on plates with LWU. Pictures of a representative experiment at day 2 are shown.

trehalose-6-phosphate phosphatase (TPP) encoded by *tps2*. Inactivation of *tps1* causes an absence of trehalose accumulation but also a growth arrest when glucose or fructose that is rapidly fermented is used as a carbon source (24). The expression of the *E. coli otsA* gene was shown to partially restore the growth of a yeast *tps1* mutant in the presence of fermentable sugars (29). Since we also wanted to quantify Tre6P production, we decided to test for complementation by *ripTPS* using the *tps1 tps2* double mutant strain, which has the same growth defect on fructose as the single *tps1* mutant, i.e., it is unable to grow on fructose but remains able to grow on galactose (30). When the *tps1 tps2* mutant strain was transformed with *ripTPS*, growth on fructose was restored to the wild-type level (Fig. 3). Similar results were observed with the expression of the *E. coli otsA* gene, as previously described (29). Complementation of the growth defect of the yeast *tps1 tps2* mutant on fructose was a first indication that *ripTPS* encodes a functional TPS.

RipTPS catalyzes Tre6P synthesis. We then used the double *tps1 tps2* mutant to test for Tre6P accumulation upon the expression of *ripTPS*. In this double mutant, the overaccumulation of Tre6P is easier to monitor in the absence of the TPS gene-encoded TPP activity. Tre6P production was quantified in the *tps1 tps2* mutant yeast strain complemented by *ripTPS* after being triggered by a glucose pulse (31). Within 5 min after the pulse, Tre6P synthesis reached a maximum in the RipTPS-expressing strains, whereas Tre6P production was below the detection threshold in the *tps1 tps2* mutant carrying the empty vector (Fig. 4, pVTU). Native and hemagglutinin (HA)-tagged versions of RipTPS and native *E. coli* OtsA were also generated and used to complement the *tps1 tps2* mutant strain. As for OtsA, the RipTPS-dependent

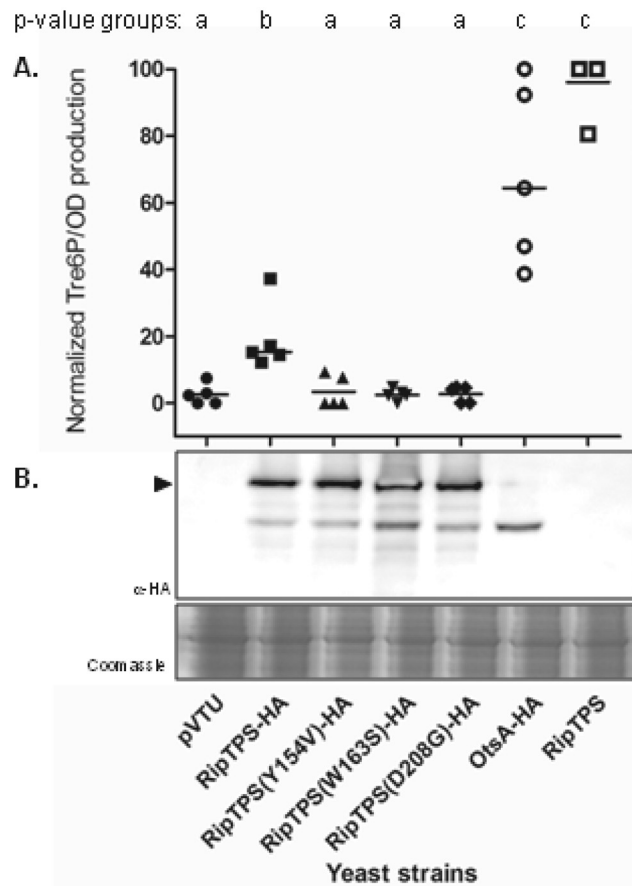


FIG 4 Production of trehalose-6-phosphate in yeast *tps1 tps2* mutant expressing *R. solanacearum ripTPS* or one of its catalytic mutants. (A) RipTPS with an HA tag and its catalytic mutants were expressed in the *tps1 tps2* yeast, and the levels of Tre6P production were compared to the levels in strains carrying an empty vector or expressing *E. coli* OtsA with an HA tag or RipTPS without a tag. All samples were analyzed five times, generating biologically independent replicates. The *P* value groupings indicate which strains cannot be distinguished (at a *P* value of <5%) using a nonparametric Wilcoxon matched-pairs signed-rank test, i.e., group a: the results for the empty vector pVTU and the three catalytic mutants cannot be distinguished and are all significantly different from the results for the other strains. (B) Western blot analysis of the expression of the HA-tagged TPS variants in the yeast protein extracts. A corresponding Coomassie-stained gel was used as a loading control. The black arrowhead indicates RipTPS (67 kDa).

production of Tre6P was confirmed, although its catalytic activity was decreased due to the addition of the HA tag.

Based on the crystal structure of *E. coli* OtsA (26) and on the model generated for *Magnaporthe grisea* TPS1 (32), conserved residues in the glucose-6-phosphate binding domain were identified and shown to be essential for activity. Corresponding nucleotide changes were introduced into the full-length *ripTPS* gene to generate 3 amino acid substitutions at these key positions (Fig. 1B; also Fig. S1 in the supplemental material). As shown in Fig. 4, the *tps1 tps2* mutant strains carrying the resulting *ripTPS*^{Y154V} (*ripTPS* with a substitution of valine for tyrosine at position 154), *ripTPS*^{W163S}, or *ripTPS*^{D208G} allele were all unable to synthesize Tre6P (the production of Tre6P was indistinguishable from that in the strain carrying the pVTU empty vector), showing the importance of these residues for TPS activity. Western blot analysis

confirmed that the wild-type RipTPS and variant alleles were produced in equal amounts in yeast (Fig. 4B). A positive HA band at 58 kDa, as shown in Fig. 4B, suggests that, in yeast, there could be cleavage of the N-terminal extension of RipTPS-HA. As expected, none of the three mutated *ripTPS* alleles restored yeast growth on fructose when introduced into the *tps1 tps2* mutant (Fig. 3).

RipTPS elicits an HR-like response on *Nicotiana tabacum* independent of TPS activity. In order to determine the contribution of *ripTPS* in *R. solanacearum* pathogenicity, a disruption mutant was created by inserting an interposon into the *ripTPS* coding sequence. The capacity of the corresponding mutant strain to cause disease was evaluated on several host plants, and no difference in symptom development was detected compared to that of the wild-type strain (see Fig. S2 in the supplemental material). Further inoculation tests on a panel of *Arabidopsis* ecotypes and competitive index experiments (13) on tomato and bean did not show any difference either (data not shown). We then wanted to evaluate the role of TPS activity during infection by *R. solanacearum* by testing available transgenic *Arabidopsis* plants expressing *E. coli otsA* (33) or *ripTPS*, generated by ourselves. Both *otsA*- and *ripTPS*-expressing plants had stunted growth and very low fertility (33; also our unpublished data), making the test of the contribution of TPS to disease difficult to evaluate.

We then investigated whether the expression of *ripTPS* could elicit defense responses in other plants. We used an *Agrobacterium*-mediated transient expression assay after infiltration of leaf mesophyll tissues using a vector carrying the full-length *ripTPS* coding sequence under the control of the 35S promoter. On *Nicotiana tabacum*, a strong HR-like necrotic response could be observed 48 h postinfiltration (Fig. 5B, a). This response could be specific to *N. tabacum*, since no reaction was observed after leaf infiltration of *Nicotiana benthamiana* or *Nicotiana glauca* (data not shown). The kinetics of this necrotic response on *N. tabacum* was comparable to the HR response elicited by the *ripAA* (*avrA*) avirulence gene product under the same experimental conditions (Fig. 5B, g) (18). Altogether, these data suggest that RipTPS is specifically recognized by the *N. tabacum* immune system.

Agrobacterium-mediated transient expression assays were also performed with strains expressing RipTPS carrying single point mutations in the essential catalytic sites described above. *Agrobacterium tumefaciens* strain GV3101::pMP90RK containing the pAM-PAT plasmids in which the *ripTPS*^{Y154V}, *ripTPS*^{W163S}, and *ripTPS*^{D208G} alleles were cloned induced an HR-like response similar to that induced by the strain carrying the wild-type *ripTPS* gene (Fig. 5B, b, c, and d). This demonstrates that the enzymatic activity of RipTPS is not required for the elicitation of the necrotic response on *N. tabacum*.

The C-terminal half of RipTPS is sufficient to trigger the HR-like response. Since plants contain TPS enzymes (34), which are related to prokaryotic TPS (Fig. 2), the finding that RipTPS elicited an HR-like response on a tobacco species was intriguing. We therefore performed *Agrobacterium*-mediated transient expression assays using the full-length *E. coli otsA* as performed for *ripTPS*. Although *otsA* is closely related to *ripTPS* (Fig. 2; also Fig. S1 in the supplemental material), we can see from the results shown in Fig. 5 (Fig. 5B, e) that *Agrobacterium*-mediated expression of *otsA* did not induce a necrotic response on *N. tabacum*.

The three functional domains of RipTPS (the T3SS translocation domain, the glucose-6-phosphate binding domain, and the

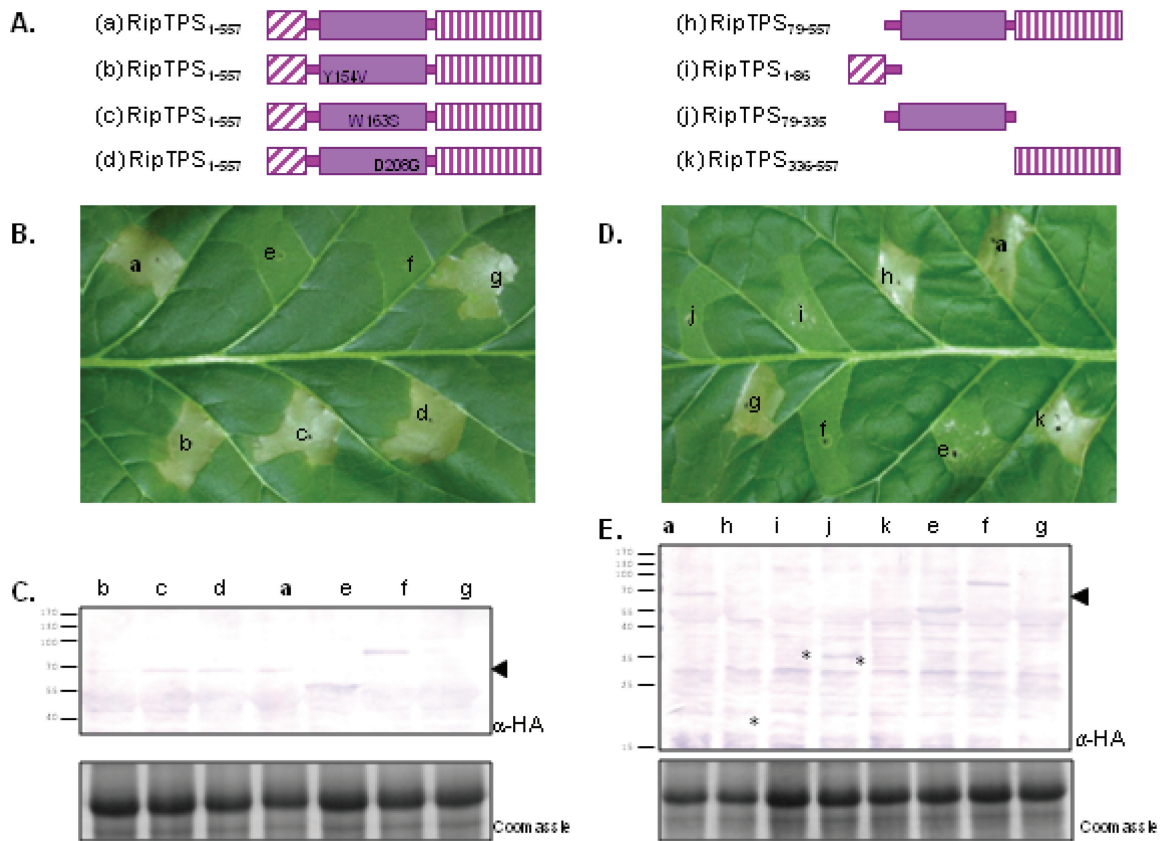


FIG 5 *Agrobacterium*-mediated transient expression of RipTPS or the C-terminal domain of RipTPS in *N. tabacum* leaves elicits an HR-like necrotic response. (A) Schematics of the structures of the RipTPS proteins expressed, including WT RipTPS (a) and the three catalytic mutants of RipTPS-HA (b, c, and d). Non-RipTPS proteins used in the experiments are not depicted; these were OtsA-HA (e), GUS-HA (negative control) (f), and AvrA (positive HR control) (g). (B and D) *N. tabacum* leaf pictures taken 3 days after infiltration of *Agrobacterium* strains, allowing the expression of the different recombinant proteins. (C and E) Western blotting with anti-HA antibody and Coomassie staining of the protein extracts from leaves infiltrated like those shown in panels B and D, respectively. The black arrowheads indicate RipTPS (67 kDa). The asterisks indicate protein that is visible but at low abundance.

UDP-glucose binding domain) (Fig. 5A) were cloned in a plant expression vector and used for transient expression assays. A necrotic response is observed only when the RipTPS C-terminal domain is present in the agroinfiltrated protein (Fig. 5D, a, h, and k). We can thus hypothesize that the *N. tabacum* immune system recognizes the C-terminal domain of RipTPS, containing the UDP-glucose binding domain. It is notable that, although the detection of the expressed proteins again proved difficult, the detection of agroinfiltrated recombinant proteins that failed to trigger necrosis was possible (Fig. 5E, see the small dots next to the HA-positive bands from infiltrations i and j). The expression of the different versions of recombinant RipTPS was confirmed by agroinfiltration in *N. benthamiana* leaves (see Fig. S3 in the supplemental material).

DISCUSSION

Trehalose is a nonreducing disaccharide found in many organisms, including eubacteria, fungi, insects, and plants. Although different biosynthetic routes exist in bacteria, a general pathway involving the successive action of TPS and TPP enzymes is conserved in fungi, plants, and many bacteria (35). Phylogenetic analyses have shown that there is a close evolutionary relationship between the TPS and TPP modules in these diverse organisms; in bacteria, the corresponding *otsA* and *otsB* genes are clustered and

are generally transcribed from a single promoter (35). *ripTPS*, while being conserved in taxonomically distant *R. solanacearum* strains (4), is never associated with a TPP gene module. Instead, the neighboring gene to *ripTPS* is *ripAV*, which encodes a T3E of unknown function (4). The presence of an N-terminal T3SS secretion domain is also unique among bacterial TPS enzymes. For RipTPS, this N-terminal extension is a functional T3SS signal, and its presence in TPS enzymes of other plant-pathogenic bacteria makes them good candidates for also being secreted effectors. This unusual modular architecture of a T3SS-dependent TPS enzyme suggests that this effector evolved from a shuffling process that Stavrinides and colleagues have called “terminal reassortment” (36). This evolutionary mechanism has been described for several bacterial effector proteins in which the termini of the effector reassort with other genetic information to create new chimeric proteins with added secretion function.

There are increasing numbers of reports in the literature indicating that trehalose metabolism emerges in the establishment of virulence traits in distantly related microbial species (37). Either in prokaryotes or in several fungal species, trehalose-associated mechanisms have been shown to contribute to cell morphogenesis, cell wall integrity, regulation of metabolism, and evasion of the host immune response (32, 37, 38). For example, a recent study

has shown that the opportunistic pathogen *Pseudomonas aeruginosa* has repurposed a specific trehalose biosynthesis pathway as a virulence factor to increase its replication rate in the intercellular leaf environment (39). However, there is not just one way to tamper with this signaling in host plants, as several distinct trehalose-associated mechanisms operate to promote pathogenesis in species-specific manners (37).

This work provides evidence that RipTPS displays trehalose-6-phosphate synthase activity and is translocated into plant cells by the T3SS. Although Tre6P is present in trace abundance in plant cells, its content is tightly regulated and not merely restricted to trehalose synthesis (34). Several studies in recent years have indeed unraveled the role of Tre6P as a key signal molecule that regulates carbon assimilation and the sugar status in plants (34, 40–43). It is therefore tempting to speculate that the pathogen directly induces Tre6P synthesis during the course of infection to subvert plant cell metabolism through modulation of the endogenous Tre6P content rather than to stimulate trehalose biosynthesis. Tre6P has many physiological effects and probable targets in plants, and the regulatory mechanisms are not yet completely understood. However, Tre6P in plants was shown to inhibit Snf1-related kinase 1 (SnRK1) activity (40), and it also indirectly increases the expression of the abscisic acid-insensitive-4 (ABI4) transcription factor (35). SnRK1 is the plant ortholog of SNF1 from yeast, and both are important regulators of sugar metabolism (44, 45). Interestingly, *Arabidopsis* SnRK1 was shown to be targeted by the *Xanthomonas campestris* T3E AvrBsT (46) and the SnRK1 homolog AKIN1 from *N. benthamiana* was shown to be targeted by two geminivirus proteins (47), suggesting that down-regulation of SnRK1 activity could be a strategy common to different plant pathogens. The fact that *ripTPS* is dispensable for *R. solanacearum* pathogenicity, as well as the multiple effects induced by Tre6P in plant cells, hampers elucidation of the biological impact of RipTPS on plant physiology that is relevant during infection. Manipulation of plant Tre6P levels could promote either plant defense suppression or, alternatively, a metabolic priming that is beneficial for the pathogen, as recently evidenced with other effectors (48–50). Even though we have not pinpointed it experimentally, we cannot exclude a contribution by RipTPS to the pathogenicity. Indeed, the absence of an apparent role could actually be yet another example of a functional overlap between unrelated effectors. Furthermore, since the *R. solanacearum* infection process involves multiple distinct steps, from root entry to xylem vessel colonization, a future challenge will be to address whether RipTPS is required at certain specific stages of this process.

Transient expression assays in tobacco revealed that RipTPS elicits strong necrosis in *N. tabacum* but not in two other tobacco species tested (*N. glutinosa* and *N. benthamiana*). This host specificity is suggestive of a hypersensitive response (HR) phenomenon. The observation that an *R. solanacearum* *ripPI ripAA* (*popPI avrA*) double mutant is HR negative on *N. tabacum* (18) also suggests that this probable HR-eliciting activity of RipTPS is suppressed by additional T3E(s) in the wild-type GMI1000 strain. Our results showed that this phenotype is independent of Tre6P synthesis. Moreover, we were able to demonstrate that this HR-like eliciting activity is associated with the RipTPS C-terminal domain. Amino acid comparison of this domain with *E. coli* OtsA (which does not elicit the plant reaction) reveals that they display 42% identity (62% similarity), with the most divergent region

corresponding to the 40-aa C-terminal end, which is only 15% identical between OtsA and RipTPS (see Fig. S1 in the supplemental material). Despite a probable common tridimensional folding of these TPS enzymes, the recognition of RipTPS by a plant immunity component might therefore be associated with some of these sequence differences. Further studies aimed at characterizing the various *ripTPS* alleles from diverse strains from the *R. solanacearum* species complex may identify *ripTPS* variants that are unable to elicit the HR-like response on *N. tabacum*. This could enable the identification of the sequence determinants actually triggering the plant response.

Many T3SS-translocated effectors mimic eukaryotic proteins in structure and function. Most often, for T3E enzymes where the molecular function was elucidated, the enzymatic activity of these T3E proteins consists of posttranslational modifications of host proteins (e.g., phosphorylation, acetylation, ubiquitination, sumoylation, etc.) or the direct degradation of host components (through hydrolase or protease activities, for example) (9, 19, 51–53). RipTPS appears to be a so-far unique example of a T3E directing the synthesis of an endogenous signal molecule in individual host cells.

Despite considerable progress during the last decade, the role of Tre6P as a regulatory factor in plants is far from being fully understood. The finding that a bacterial pathogen could induce the production of Tre6P in plant cells further highlights the importance of this metabolite in the molecular physiology of plants.

MATERIALS AND METHODS

Bacterial strains, yeast strains, plasmids, growth conditions, and plant material. The bacterial and yeast strains and plasmids used for this study are described in Table S1 in the supplemental material. *Escherichia coli* cells were grown in Luria-Bertani medium at 37°C with 100 µg/ml ampicillin or 15 µg/ml gentamycin. *Agrobacterium tumefaciens* strain GV3101::pMP90RK cells were grown in YEB medium (5 g/liter beef extract, 1 g/liter yeast extract, 5 g/liter peptone, 5 g/liter sucrose, 2 mM MgSO₄, pH 7.2) at 28°C with 100 µg/ml rifampin, 50 µg/ml kanamycin, 15 µg/ml gentamicin, and 75 µg/ml carbenicillin. Agar was added at 1.5% (wt/vol) for solid medium. *R. solanacearum* strains GMI1000, GMI1694 (*hrcV*, a T3SS mutant derivative), and GRS432 (*ripTPS* mutant) were grown in complete medium B or minimal medium (MM) at 28°C with or without 40 µg/ml spectinomycin (54). For liquid cultures, spectinomycin was reduced by half. The *S. cerevisiae* *tps1 tps2* mutant strain YSH652 (*MATα leu2-3,112 ura3-1 trp1-1 his3-11,15 ade2-1 can1-100 tps1::TRP1 tps2::LEU2 GAL SUC*) and the control strain W303-1A (*MATα leu2-3,112 ura3-1 trp1-1 his3-11,15 ade2-1 can1-100 GAL SUC*) were grown at 30°C in SD-LWU and SD medium (both from Clontech), respectively, supplemented with galactose unless otherwise stated. The plants used in this study were *Nicotiana tabacum* cv. Bottom special, *Nicotiana benthamiana*, eggplant (*Solanum melongena* cv. Zebrina), tomato (*Solanum lycopersicum* cv. Marmande), and geranium (*Geranium sanguineum* var. Maverick Ecarlate), grown in the greenhouse, and *Arabidopsis thaliana* grown in a growth chamber at 22°C with a 9-h day length.

DNA manipulations and genetic constructs. Constructs were created using the Gateway technology as recommended by the manufacturer (Life Technologies, Carlsbad, CA). *ripTPS* was cloned from the genomic DNA of *R. solanacearum* GMI1000 in pDONR207, creating pMP12 (with a stop codon) and pMP15 (without a stop codon). Amplifications were performed in two steps, using the cloning primers (731GW-ATG and 731GW-STOP or 731GW-NOSTOP) in the first PCR and then universal primers (attB1 and attB2) in the second PCR, with Platinum Pfx (Life Technologies), Pfu Ultra (StrataGen, Kirkland, WA), or Phusion (NEB, Ipswich, MA). The primers used for the amplifications are provided in Table S1 in the supplemental material. The three mutant alleles of *ripTPS*

were generated using the QuikChange XL site-directed mutagenesis kit (Agilent) on the pMP15 plasmid, creating plasmids pMP90 (Y154V), pMP91 (W163S), and pMP92 (D208G), respectively. Expression plasmids (pMP72, pMP93, pMP94, and pMP95) were created by LR Gateway cloning using pAM-PAT-P35S-GW-3xHA (L. D. Noël and J. E. Parker, unpublished data) and used to transform *Agrobacterium tumefaciens* GV3101::pMP90RK. The different constructs derived from RipTPS (RipTPS_{79–557}, RipTPS_{1–86}, RipTPS_{79–335}, and RipTPS_{336–557}) were generated by PCR (using primer pairs oMP1-oMP3, 731GW-ATG-oMP4, oMP1-oAuA7, and oAuA5-oMP3, respectively) (Table S1) and cloned in the pDONR207 vector (pMP71, pMP35, pACC758, and pMP87) and then in pAM-PAT-P35S-GW-3xHA (pMP73, pACC678, pACC766, and pMP89), and the resulting plasmids were used to transform *A. tumefaciens*. The expression levels of GUS (courtesy of L. Deslandes), OtsA (pMP74), and AvrA (pMP99) (18) were used as controls for the *A. tumefaciens* assay. OtsA from *E. coli* was amplified using primers otsA-fwd and otsA-rev (Table S1).

Construction of an *ripTPS* mutant strain. *ripTPS* was disrupted by the insertion of an Ω cassette conferring resistance to spectinomycin as previously described (55). A 2.2-kb DNA fragment comprising the *ripTPS* coding sequence was cloned after PCR amplification using primers GRS432 fwd and GRS432 Rev. The Ω cassette was inserted into the unique EcoRI restriction site within the coding sequence, resulting in plasmid pMP2. This construct was linearized by NcoI and introduced into *R. solanacearum* GMI1000 by natural transformation. The mutant strain GRS432 generated after selection for a double recombination event using spectinomycin resistance and was further checked by PCR.

Adenylate cyclase assay. A DNA fragment comprising 509 bp upstream from the *ripTPS* start codon and the region encoding the first 83 amino acids was PCR amplified (primers BglII731 and HindIII731) (see Table S1 in the supplemental material) and cloned into the pSC266 vector (6) HindIII-BglII restriction sites to create a translational fusion with the *cyoA'* gene. The resulting plasmid, named pGG7, was introduced into the GMI1000 and GMI1694 strains by natural transformation to select for a single recombination event, leading to genomic integration. Natural transformation of *R. solanacearum* strains was performed after growth in minimal medium supplemented with 2% glycerol as described previously (54).

The adenylate cyclase assay was performed as previously described (6). Briefly, strain GMI1000 and derivatives carrying plasmid pGG7 were infiltrated into *Nicotiana tabacum* leaves at an optical density (OD) of 1. Plants were sampled 7 h later with a cork borer. Leaf disks were transferred into Eppendorf tubes and immediately frozen in liquid nitrogen. For cyclic AMP (cAMP) extraction, samples in Eppendorf tubes were kept frozen while grinding by shaking with 2-mm tungsten beads in a Qiagen MM300 mixer mill for two runs of 2 min at 30 Hz. Samples were stored at -80°C before cAMP quantification. Protein concentration was assessed with the Bio-Rad protein assay kit. Cyclic AMP levels were monitored with a cAMP enzyme immunoassay kit (Biotrak; Amersham Pharmacia Biotech) according to the manufacturer's instructions.

Complementation of the *tps1 tps2* yeast mutant. To express *ripTPS* and its derivatives in yeast, the Gateway-compatible yeast episomic vector pVTU102-GW containing the yeast alcohol dehydrogenase (ADH1) gene promoter (56) was used. The full-length *ripTPS* gene was cloned, resulting in the yeast expression plasmid named pMP31, which was used to transform the *tps1 tps2* yeast mutant strain (31). Similarly, the catalytic mutants of *ripTPS* were cloned in pVTU102-GW (pMP96, pMP97, and pMP98). To create the HA-tagged versions of these vectors, a PCR fragment obtained from pMP72 amplification with primers TPSHA-fwd and TPSHA-rev (see Table S1 in the supplemental material) was inserted into the XhoI-HindIII site. The resulting plasmids (pMP104, pMP105, pMP106, and pMP107) were used to transform the *tps1 tps2* mutant yeast strain. As a positive control, the full-length *otsA* gene from *E. coli* was cloned in the pVTU102-GW vector with an HA tag in the Sall-HindIII site (pMP108), using primers otsAHA-fwd and otsAHA-rev (Table S1).

The yeast strains were grown on SD-LWU containing 2% galactose and 40 mg/liter adenine. For the fructose growth assay, 10-fold dilution series from exponential growing cells were spotted onto plates containing either fructose or galactose.

To measure the production of Tre6P, the extraction of yeast metabolites following a glucose pulse was carried out as described previously (31). The measured production of Tre6P (mM Tre6P/OD unit) was normalized by attributing a value of 100 to the sample with maximal value. All the samples were analyzed five times, generating independent biologically replicates. To analyze the differences between strains, we used the non-parametric Wilcoxon matched-pairs signed-rank test with a one-tailed *P* value. This was performed using the GraphPad Prism 5.0 software package.

Pathogenicity assays. *Arabidopsis* (Col-0) plantlets were grown for 4 to 5 weeks on Jiffy plugs (Jiffy Products International BV, Netherlands). Geranium (*Geranium sanguineum* var. Maverick Ecarlate), tomato (cv. Marmande), and eggplant (cv. Zebrina) were grown in greenhouse facilities in potting mixture. For all plant inoculations, the roots were soaked with a bacterial suspension at 10^7 CFU/ml of GMI1000 or GRS432 (the *ripTPS* mutant). Solanaceae were then placed at 28°C (light) and 27°C (night) with a 12-h photoperiod. For *Arabidopsis*, the temperatures were 27°C (light) and 26°C (night). The progression of the disease was reported by scoring the plants on a scale from 1 to 4 based on 25% to 100% of leaves being wilted; to perform the survival analysis (see Fig. S2 in the supplemental material), all scores equal to or higher than 2 (50% wilted leaves) were set as 1 (or dead) when the lower scores were 0 (or alive). The experiments were repeated at least 3 times independently. The statistical analysis was performed as described previously (21).

***Agrobacterium*-mediated expression of proteins in plant cells.** *A. tumefaciens* strains carrying plasmid-borne *ripTPS* constructs were grown overnight in YEB medium. Cells were pelleted at 4,000 rpm, resuspended in infiltration medium (10 mM MgCl_2 , 10 mM morpholine ethanesulfonic acid, and 150 μM acetosyringone), and incubated for 2 h at room temperature. Resuspended cells were infiltrated into leaves of 4-week-old *Nicotiana* spp. plants at an optical density at 600 nm (OD_{600}) of 0.6 with a 1-ml needleless syringe. The infiltrated plants were incubated in growth chambers for a 16-h day at 20°C . After infiltration (48 to 72 h), leaf disks taken in infiltrated areas were ground with a mixer mill (MM400; Retsch, Haan, Germany) and homogenized in Laemmli buffer in order to be analyzed by Western blotting to control for the expression levels. Rat anti-HA antibody (1:5,000) (number 11867423001; Roche) was incubated overnight in Tris-buffered saline (TBS)--0.1% Tween with 1% bovine serum albumin (BSA), and then goat anti-rat antibody coupled to alkaline phosphatase (1:10,000) (A8438; Sigma) was added after three washes of 10 min each in TBS-Tween, and the mixture was incubated for 1 h. Incubation was followed by two washes in TBS-Tween and then nitroblue tetrazolium (NBT)-BCIP (5-bromo-4-chloro-3-indolylphosphate)-based staining. The expression of the RipTPS variants was followed in *N. benthamiana* in parallel to the expression in *N. tabacum* because the low expression level in *N. tabacum* was limiting for Western blot analysis. After SDS-PAGE electrophoresis, Coomassie staining was performed to check for equal protein loading (57).

SUPPLEMENTAL MATERIAL

Supplemental material for this article may be found at <http://mbio.asm.org/lookup/suppl/doi:10.1128/mBio.02065-14/-DCSupplemental>.

Figure S1, EPS file, 0.8 MB.

Figure S2, EPS file, 0.2 MB.

Figure S3, EPS file, 0.04 MB.

Table S1, XLSX file, 0.02 MB.

ACKNOWLEDGMENTS

We thank Audrey Anglade (LIPM), Sebastien Cunnac (LIPM), Aurelie Vax (LISBP), and Marie-Odile Loret (LISBP) for their help in several experiments. We also thank Jean-Luc Pariente (LIPM), Claudette Icher

(LIPM), and Céline Remblière (LIPM) for the production of the plant material.

This work was supported by the French Laboratory of Excellence project TULIP (ANR-10-LABX-41 and ANR-11-IDEX-0002-02) and by a grant from the Ministère de l'Enseignement Supérieur et de la Recherche to M.P. This work was supported in part by a grant from ANR (ANR-07-Blan-0205-01) and by a grant from Région Midi-Pyrénées (grant no. 07005583) to J.M.F.

REFERENCES

- Genin S, Denny TP. 2012. Pathogenomics of the *Ralstonia solanacearum* species complex. *Annu. Rev. Phytopathol.* 50:67–89. <http://dx.doi.org/10.1146/annurev-phyto-081211-173000>.
- Peeters N, Guidot A, Vaillau F, Valls M. 2013. *Ralstonia solanacearum*, a widespread bacterial plant pathogen in the post-genomic era. *Mol. Plant Pathol.* 14:651–662. <http://dx.doi.org/10.1111/mpp.12038>.
- Genin S. 2010. Molecular traits controlling host range and adaptation to plants in *Ralstonia solanacearum* species complex. *New Phytol.* 187:920–928. <http://dx.doi.org/10.1111/j.1469-8137.2010.03397.x>.
- Peeters N, Carrère S, Anisimova M, Plener L, Cazalé AC, Genin S. 2013. Répertoire, unifié nomenclature and evolution of the type III effector gene set in the *Ralstonia solanacearum* species complex. *BMC Genomics* 14:859. <http://dx.doi.org/10.1186/1471-2164-14-859>.
- Mukaihara T, Tamura N, Iwabuchi M. 2010. Genome-wide identification of a large repertoire of *Ralstonia solanacearum* type III effector proteins by a new functional screen. *Mol. Plant Microbe Interact.* 23:251–262. <http://dx.doi.org/10.1094/MPMI-23-3-0251>.
- Cunnac S, Occhialini A, Barberis P, Boucher C, Genin S. 2004. Inventory and functional analysis of the large Hrp regulon in *Ralstonia solanacearum*: identification of novel effector proteins translocated to plant host cells through the type III secretion system. *Mol. Microbiol.* 53:115–128. <http://dx.doi.org/10.1111/j.1365-2958.2004.04118.x>.
- Deslandes L, Genin S. 2014. Opening the *Ralstonia solanacearum* type III effector tool box: insights into host cell subversion mechanisms. *Curr. Opin. Plant Biol.* 20:110–117.
- Cunnac S, Boucher C, Genin S. 2004. Characterization of the *cis*-acting regulatory element controlling HrpB-mediated activation of the type III secretion system and effector genes in *Ralstonia solanacearum*. *J. Bacteriol.* 186:2309–2318. <http://dx.doi.org/10.1128/JB.186.8.2309-2318.2004>.
- Angot A, Peeters N, Lechner E, Vaillau F, Baud C, Gentsbittel L, Sartorel E, Genschik P, Boucher C, Genin S. 2006. *Ralstonia solanacearum* requires F-box-like domain-containing type III effectors to promote disease on several host plants. *Proc. Natl. Acad. Sci. U. S. A.* 103:14620–14625. <http://dx.doi.org/10.1073/pnas.0509393103>.
- Jacobs JM, Milling A, Mitra RM, Hogan CS, Ailloud F, Prior P, Allen C. 2013. *Ralstonia solanacearum* requires PopS, an ancient AvrE-family effector, for virulence and to overcome salicylic acid-mediated defenses during tomato pathogenesis. *mBio* 4(6):e00875-13. <http://dx.doi.org/10.1128/mBio.00875-13>.
- Chen L, Shiota M, Zhang Y, Kiba A, Hikichi Y, Ohnishi K. 2014. Involvement of HLK effectors in *Ralstonia solanacearum* disease development in tomato. *J. Gen. Plant Pathol.* 80:79–84. <http://dx.doi.org/10.1007/s10327-013-0490-2>.
- Solé M, Popa C, Mith O, Sohn KH, Jones JD, Deslandes L, Valls M. 2012. The *avr* gene family encodes a novel class of *Ralstonia solanacearum* type III effectors displaying virulence and avirulence activities. *Mol. Plant Microbe Interact.* 25:941–953. <http://dx.doi.org/10.1094/MPMI-12-11-0321>.
- Macho AP, Guidot A, Barberis P, Beuzón CR, Genin S. 2010. A competitive index assay identifies several *Ralstonia solanacearum* type III effector mutant strains with reduced fitness in host plants. *Mol. Plant Microbe Interact.* 23:1197–1205. <http://dx.doi.org/10.1094/MPMI-23-9-1197>.
- Jones JD, Dangl JL. 2006. The plant immune system. *Nature* 444:323–329. <http://dx.doi.org/10.1038/nature05286>.
- Lavie M, Shillington E, Eguluz C, Grimsley N, Boucher C. 2002. PopP1, a new member of the YopJ/AvrRxv family of type III effector proteins, acts as a host-specificity factor and modulates aggressiveness of *Ralstonia solanacearum*. *Mol. Plant Microbe Interact.* 15:1058–1068. <http://dx.doi.org/10.1094/MPMI.2002.15.10.1058>.
- Deslandes L, Olivier J, Peeters N, Feng DX, Khounlotham M, Boucher C, Somssich I, Genin S, Marco Y. 2003. Physical interaction between RRS1-R, a protein conferring resistance to bacterial wilt, and PopP2, a type III effector targeted to the plant nucleus. *Proc. Natl. Acad. Sci. U. S. A.* 100:8024–8029. <http://dx.doi.org/10.1073/pnas.1230660100>.
- Nahar K, Matsumoto I, Taguchi F, Inagaki Y, Yamamoto M, Toyoda K, Shiraihi T, Ichinose Y, Mukaihara T. 2014. *Ralstonia solanacearum* type III secretion system effector Rip36 induces a hypersensitive response in the nonhost wild eggplant *Solanum torvum*. *Mol. Plant Pathol.* 15:297–303. <http://dx.doi.org/10.1111/mpp.12079>.
- Poueymiro M, Cunnac S, Barberis P, Deslandes L, Peeters N, Cazale-Noel AC, Boucher C, Genin S. 2009. Two type III secretion system effectors from *Ralstonia solanacearum* GMI1000 determine host-range specificity on tobacco. *Mol. Plant Microbe Interact.* 22:538–550. <http://dx.doi.org/10.1094/MPMI-22-5-0538>.
- Tasset C, Bernoux M, Jauneau A, Pouzet C, Brière C, Kieffer-Jacquiod S, Rivas S, Marco Y, Deslandes L. 2010. Autoacetylation of the *Ralstonia solanacearum* effector PopP2 targets a lysine residue essential for RRS1-R-mediated immunity in Arabidopsis. *PLoS Pathog.* 6:e1001202. <http://dx.doi.org/10.1371/journal.ppat.1001202>.
- Kajava AV, Anisimova M, Peeters N. 2008. Origin and evolution of GALA-LRR, a new member of the CC-LRR subfamily: from plants to bacteria? *PLoS One* 3:e1694. <http://dx.doi.org/10.1371/journal.pone.0001694>.
- Remigi P, Anisimova M, Guidot A, Genin S, Peeters N. 2011. Functional diversification of the GALA type III effector family contributes to *Ralstonia solanacearum* adaptation on different plant hosts. *New Phytol.* 192:976–987. <http://dx.doi.org/10.1111/j.1469-8137.2011.03854.x>.
- Li L, Atef A, Piatek A, Ali Z, Piatek M, Aouida M, Sharakuu A, Mahjoub A, Wang G, Khan S, Fedoroff NV, Zhu J-K, Mahfouz MM. 2013. Characterization and DNA-binding specificities of *Ralstonia solanacearum* TAL-like effectors. *Mol. Plant* 6:1318–1330. <http://dx.doi.org/10.1093/mp/sst006>.
- De Lange O, Schreiber T, Schandry N, Radeck J, Braun KH, Koszowski J, Heuer H, Strauss A, Lahaye T. 2013. Breaking the DNA-binding code of *Ralstonia solanacearum* TAL effectors provides new possibilities to generate plant resistance genes against bacterial wilt disease. *New Phytol.* 199:773–786. <http://dx.doi.org/10.1111/nph.12324>.
- Lunn JE, Delorge I, Figueroa CM, Van Dijk P, Stitt M. 2014. Trehalose metabolism in plants. *Plants J.* 79:544–567. <http://dx.doi.org/10.1111/tpl.12509>.
- Gibson RP, Tarling CA, Roberts S, Withers SG, Davies GJ. 2004. The donor subsite of trehalose-6-phosphate synthase: binary complexes with UDP-glucose and UDP-2-deoxy-2-fluoro-glucose at 2 Å resolution. *J. Biol. Chem.* 279:1950–1955. <http://dx.doi.org/10.1074/jbc.M307643200>.
- Gibson RP, Turkenburg JP, Charnock SJ, Lloyd R, Davies GJ. 2002. Insights into trehalose synthesis provided by the structure of the retaining glucosyltransferase OtsA. *Chem. Biol* 9:1337–1346.
- Sory MP, Cornelis GR. 1994. Translocation of a hybrid YopE-adenylate cyclase from *Yersinia enterocolitica* into HeLa cells. *Mol. Microbiol.* 14:583–594. <http://dx.doi.org/10.1111/j.1365-2958.1994.tb02191.x>.
- Remenant B, de Cambiaire JC, Cellier G, Jacobs JM, Mangenot S, Barbe V, Lajus A, Vallenet D, Medigue C, Fegan M, Allen C, Prior P. 2011. *Ralstonia solanacearum*, the blood disease bacterium and some Asian *R. solanacearum* strains form a single genomic species despite divergent lifestyles. *PLoS One* 6:e24356. <http://dx.doi.org/10.1371/journal.pone.0024356>.
- Bonini BM, Van Vaecck C, Larsson C, Gustafsson L, Ma P, Winderickx J, Van Dijk P, Thevelein JM. 2000. Expression of *Escherichia coli* otsA in a *Saccharomyces cerevisiae* tps1 mutant restores trehalose 6-phosphate levels and partly restores growth and fermentation with glucose and control of glucose influx into glycolysis. *Biochem. J.* 350:261–268. <http://dx.doi.org/10.1042/0264-6021:3500261>.
- Walther T, Mtmet N, Alkim C, Vax A, Loret MO, Ullah A, Gancedo C, Smits GJ, François JM. 2013. Metabolic phenotypes of *Saccharomyces cerevisiae* mutants with altered trehalose 6-phosphate dynamics. *Biochem. J.* 454:227–237. <http://dx.doi.org/10.1042/BJ20130587>.
- Loret MO, Pedersen L, François J. 2007. Revised procedures for yeast metabolites extraction: application to a glucose pulse to carbon-limited yeast cultures, which reveals a transient activation of the purine salvage pathway. *Yeast* 24:47–60. <http://dx.doi.org/10.1002/yea.1435>.
- Wilson RA, Jenkinson JM, Gibson RP, Littlechild JA, Wang ZY, Talbot NJ. 2007. Tps1 regulates the pentose phosphate pathway, nitrogen metabolism and fungal virulence. *EMBO J.* 26:3673–3685. <http://dx.doi.org/10.1038/sj.emboj.7601795>.
- Schluepman H, Pellny T, van Dijken A, Smeekens S, Paul M. 2003. Trehalose 6-phosphate is indispensable for carbohydrate utilization and

- growth in *Arabidopsis thaliana*. *Proc. Natl. Acad. Sci. U. S. A.* 100: 6849–6854. <http://dx.doi.org/10.1073/pnas.1132018100>.
34. Paul MJ, Primavesi LF, Jhurrea D, Zhang Y. 2008. Trehalose metabolism and signaling. *Annu. Rev. Plant Biol.* 59:417–441. <http://dx.doi.org/10.1146/annurev.arplant.59.032607.092945>.
 35. Avonce N, Mendoza-Vargas A, Morett E, Iturriaga G. 2006. Insights on the evolution of trehalose biosynthesis. *BMC Evol. Biol.* 6:109. <http://dx.doi.org/10.1186/1471-2148-6-109>.
 36. Stavrinides J, Ma W, Guttman DS. 2006. Terminal reassortment drives the quantum evolution of type III effectors in bacterial pathogens. *PLoS Pathog.* 2:e104. <http://dx.doi.org/10.1371/journal.ppat.0020104>.
 37. Tourneau H, Fiori A, Van Dijck P. 2013. Relevance of trehalose in pathogenicity: some general rules, yet many exceptions. *PLoS Pathog.* 9:e1003447.
 38. Puttikamonkul S, Willger SD, Grahl N, Perfect JR, Movahed N, Bothner B, Park S, Paderu P, Perlin DS, Cramer RA, Jr. 2010. Trehalose 6-phosphate phosphatase is required for cell wall integrity and fungal virulence but not trehalose biosynthesis in the human fungal pathogen *Aspergillus fumigatus*. *Mol. Microbiol.* 77:891–911. <http://dx.doi.org/10.1111/j.1365-2958.2010.07254.x>.
 39. Djonović S, Urbach JM, Drenkard E, Bush J, Feinbaum R, Ausubel JL, Traficante D, Risech M, Kocks C, Fischbach MA, Priebe GP, Ausubel FM. 2013. Trehalose biosynthesis promotes *Pseudomonas aeruginosa* pathogenicity in plants. *PLoS Pathog.* 9:e1003217. <http://dx.doi.org/10.1371/journal.ppat.1003217>.
 40. Zhang Y, Primavesi LF, Jhurrea D, Andralojc PJ, Mitchell RA, Powers SJ, Schlupepmann H, Delatte T, Winkler A, Paul MJ. 2009. Inhibition of SNF1-related protein kinase1 activity and regulation of metabolic pathways by trehalose-6-phosphate. *Plant Physiol.* 149:1860–1871. <http://dx.doi.org/10.1104/pp.108.133934>.
 41. Wahl V, Ponnuru J, Schlereth A, Arrivault S, Langenecker T, Franke A, Feil R, Lunn JE, Stitt M, Schmid M. 2013. Regulation of flowering by trehalose-6-phosphate signaling in *Arabidopsis thaliana*. *Science* 339: 704–707. <http://dx.doi.org/10.1126/science.1230406>.
 42. Ponnuru J, Wahl V, Schmid M. 2011. Trehalose-6-phosphate: connecting plant metabolism and development. *Front. Plant Sci.* 2:70.
 43. Schlupepmann H, Berke L, Sanchez-Perez GF. 2012. Metabolism control over growth: a case for trehalose-6-phosphate in plants. *J. Exp. Bot.* 63: 3379–3390. <http://dx.doi.org/10.1093/jxb/err311>.
 44. Hardie DG. 2007. AMP-activated/SNF1 protein kinases: conserved guardians of cellular energy. *Nat. Rev. Mol. Cell Biol.* 8:774–785. <http://dx.doi.org/10.1038/nrm2249>.
 45. Halford NG, Hey SJ. 2009. Snf1-related protein kinases (SnRKs) act within an intricate network that links metabolic and stress signalling in plants. *Biochem. J.* 419:247–259. <http://dx.doi.org/10.1042/BJ20082408>.
 46. Szczesny R, Büttner D, Escolar L, Schulze S, Seifert A, Bonas U. 2010. Suppression of the AvrBs1-specific hypersensitive response by the YopJ effector homolog AvrBsT from *Xanthomonas* depends on a SNF1-related kinase. *New Phytol.* 187:1058–1074. <http://dx.doi.org/10.1111/j.1469-8137.2010.03346.x>.
 47. Hao L, Wang H, Sunter G, Bisaro DM. 2003. Geminivirus AL2 and L2 proteins interact with and inactivate SNF1 kinase. *Plant Cell* 15: 1034–1048. <http://dx.doi.org/10.1105/tpc.009530>.
 48. Chen LQ, Hou BH, Lalonde S, Takanao H, Hartung ML, Qu XQ, Guo WJ, Kim JG, Underwood W, Chaudhuri B, Chermak D, Antony G, White FF, Somerville SC, Mudgett MB, Frommer WB. 2010. Sugar transporters for intercellular exchange and nutrition of pathogens. *Nature* 468:527–532. <http://dx.doi.org/10.1038/nature09606>.
 49. Djamei A, Schipper K, Rabe F, Ghosh A, Vincon V, Kahnt J, Osorio S, Tohge T, Fernie AR, Feussner I, Feussner K, Meinicke P, Stierhof YD, Schwarz H, Macek B, Mann M, Kahmann R. 2011. Metabolic priming by a secreted fungal effector. *Nature* 478:395–398. <http://dx.doi.org/10.1038/nature10454>.
 50. Yadav UP, Ivakov A, Feil R, Duan GY, Walther D, Giavalisco P, Piques M, Carillo P, Hubberten HM, Stitt M, Lunn JE. 2014. The sucrose-trehalose 6-phosphate (Tre6P) nexus: specificity and mechanisms of sucrose signalling by Tre6P. *J. Exp. Bot.* 65:1051–1068. <http://dx.doi.org/10.1093/jxb/ert457>.
 51. Wang Y, Li J, Hou S, Wang X, Li Y, Ren D, Chen S, Tang X, Zhou JM. 2010. A *Pseudomonas syringae* ADP-ribosyltransferase inhibits *Arabidopsis* mitogen-activated protein kinases. *Plant Cell* 22:2033–2044. <http://dx.doi.org/10.1105/tpc.110.075697>.
 52. Zhao B, Dahlbeck D, Krasileva KV, Fong RW, Staskawicz BJ. 2011. Computational and biochemical analysis of the *Xanthomonas* effector AvrBs2 and its role in the modulation of *Xanthomonas* type three effector delivery. *PLoS Pathog.* 7:e1002408. <http://dx.doi.org/10.1371/journal.ppat.1002408>.
 53. Dean P. 2011. Functional domains and motifs of bacterial type III effector proteins and their roles in infection. *FEMS Microbiol. Rev.* 35:1100–1125. <http://dx.doi.org/10.1111/j.1574-6976.2011.00271.x>.
 54. Plener L, Manfredi P, Valls M, Genin S. 2010. PrhG, a transcriptional regulator responding to growth conditions, is involved in the control of the type III secretion system regulon in *Ralstonia solanacearum*. *J. Bacteriol.* 192:1011–1019. <http://dx.doi.org/10.1128/JB.01189-09>.
 55. Plener L, Boistard P, González A, Boucher C, Genin S. 2012. Metabolic adaptation of *Ralstonia solanacearum* during plant infection: a methionine biosynthesis case study. *PLoS One* 7:e36877. <http://dx.doi.org/10.1371/journal.pone.0036877>.
 56. Pazhouhandeh M, Dieterle M, Marrocco K, Lechner E, Berry B, Brault V, Hemmer O, Kretsch T, Richards KE, Genschik P, Ziegler-Graff V. 2006. F-box-like domain in the poliovirus protein P0 is required for silencing suppressor function. *Proc. Natl. Acad. Sci. U. S. A.* 103: 1994–1999. <http://dx.doi.org/10.1073/pnas.0510784103>.
 57. Neuhoff V, Stamm R, Eibl H. 1985. Clear background and highly sensitive protein staining with Coomassie blue dyes in polyacrylamide gels: a systematic analysis. *Electrophoresis* 6:427–448. <http://dx.doi.org/10.1002/elps.1150060905>.
 58. Dereeper A, Guignon V, Blanc G, Audic S, Buffet S, Chevenet F, Dufayard J-F, Guindon S, Lefort V, Lescot M, Claverie J-M, Gascuel O. 2008. Phylogeny.fr: robust phylogenetic analysis for the non-specialist. *Nucleic Acids Res.* 36:W465–W469. <http://dx.doi.org/10.1093/nar/gkn180>.
 59. Waterhouse AM, Procter JB, Martin DMA, Clamp M, Barton GJ. 2009. Jalview, version 2. a multiple sequence alignment Editor and analysis workbench. *Bioinformatics* 25:1189–1191. <http://dx.doi.org/10.1093/bioinformatics/btp033>.